Dynamics of Electron Beam Instabilities under Conditions of Multiwave Distributed Feedback

K.G. Batrakov[1] and S.N. Sytova[2]

Institute for Nuclear Problems, Belarusan State University, 11 Bobruiskaya st., Minsk, 220050 BELARUS

E-mail: [1]batrakov@inp.minsk.by or [2]sytova@inp.minsk.by

(Received 20 May 2005)

Oscillation and amplification regimes of Volume Free Electron Laser (VFEL) operation under condition of multiwave volume distributed feedback (VDFB) are discussed. Electron beam instabilities in VFEL transfer it to regenerative amplification regime (first transition point), steady oscillation regime (second transition point), to nonstationary oscillation regime and through the series of transition points to chaos under increasing current. Nonstationary regime is characterized by changing of oscillation frequency in series of transition points. Some results are obtained analytically. Most part of results is produced by numerical simulation of nonlinear VFEL dynamics. Dependence of transition currents in transition (bifurcation) points on VFEL parameters is demonstrated.

Key words: Volume Free Electron Laser, quasi-Cherenkov instability

PACS numbers: 41.60.Cr; 35Q60, 35F20, 65M06

1 Introduction

This contribution is devoted to the analysis of non-stationary dynamics of electron beam quasi-Cherenkov instability in different realizations of VFEL with multiwave VDFB.

Conception of VFEL based on parametric (quasi-Cherenkov) beam instability was proposed firstly in [1] for generation in X-ray range. First ideas to use VDBF in VFEL was proposed in [2]. First lasing of VFEL in millimeter range based on principal ideas referred above was recently obtained by the group of Institute for Nuclear Problems [3]. Experimental work on VFEL goes on.

2 Volume distributed feedback

Volume distributed feedback can significantly enhance lasing process. For example VDFB can reduce interaction length, provide mode discrimination in overmode generating systems. Continuous variation of VDFB parameters can be used to tune lasing frequency. One of the most suitable mechanism for providing VDFB is Bragg multiwave dynamical diffraction. n-wave dynamical diffraction is realized when conditions

$$2\mathbf{k}\boldsymbol{\tau}_i + \boldsymbol{\tau}_i^2 \approx 0 \qquad (1)$$

are fulfilled for $i = 1, \ldots, (n-1)$. Here $\boldsymbol{\tau}_i = \{2\pi n_1 d_1, 2\pi n_2 d_2, 2\pi n_3 d_3\}$ is a reciprocal lattice vector, $\{d_i\}$ are spatial periods of the target, $\{n_i\}$ are integers. In this case an eigenmode has the form of n coupled waves. At least one of these waves can be in resonance condition with an electron beam. This resonance condition can be Cherenkov synchronism condition, resonance condition of oscillator and others depending on specific lasing mechanism.

In conventional design only one mode is in synchronism with the electron beam and the threshold current j is proportional to $1/(kL)^3$, where $k = \omega/c$, ω is a frequency, L is an interaction length. If two modes are in synchronism with electrons at once we have $j \sim 1/(kL)^5$ and $j \sim 1/(kL)^{3+2(n-1)}$ if n wave are in synchronism with electrons. So, threshold current can be sig-

nificantly decreased when modes are degenerated (we assume $kL \gg 1$) in multiwave diffraction geometry. On the other hand interaction length can be reduced at given current value. Simultaneous synchronism of several modes with electrons corresponds to roots degeneration of dispersion equation. Therefore a part of present work is devoted to investigation of dispersion equation and defining the region of parameters corresponding to such degeneration.

Simulation of VFEL dynamics in region of roots degeneration is fulfilled in three-wave VDFB geometry in this paper.

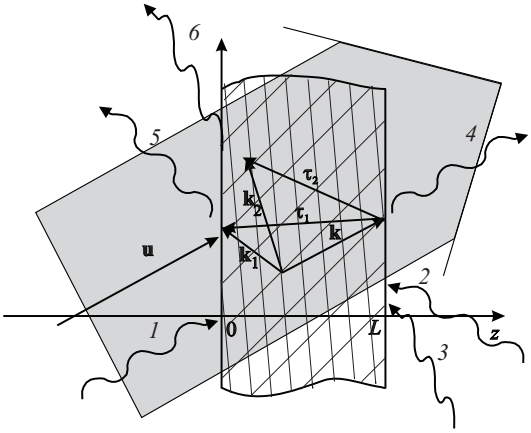

FIG. 1. Scheme of quasi-Cherenkov VFEL in Bragg-Bragg geometry

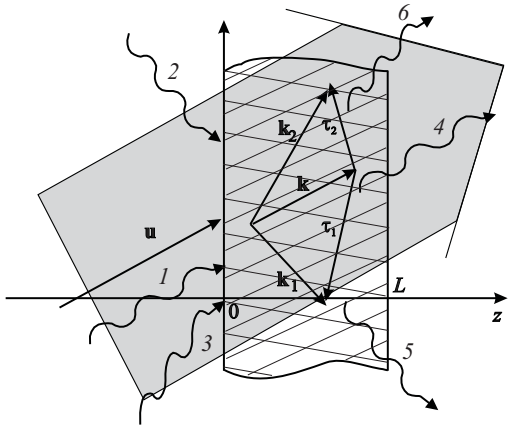

FIG. 2. Scheme of quasi-Cherenkov VFEL in Laue-Laue geometry

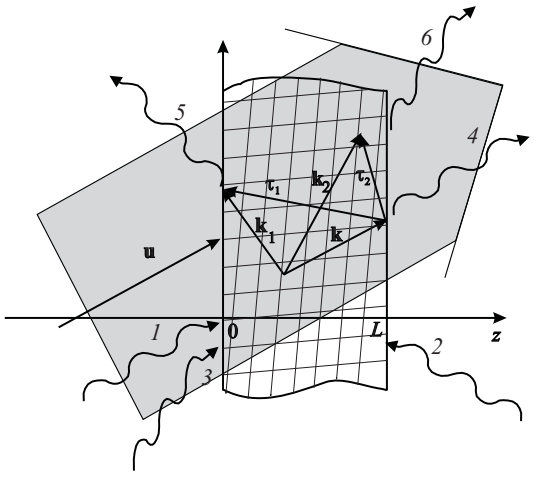

FIG. 3. Scheme of quasi-Cherenkov VFEL in Bragg-Laue geometry

3 Mathematical model of VFEL

Let us make a brief review of basic VFEL operation principles. Main feature of VDFB is multiwave distributed feedback. Wave propagation direction does not coincide with electron velocity direction in VFEL. VFEL is an oversized system (system dimensions exceed the wavelength) and VDFB fulfils very important function of mode discrimination. Electron beam in VFEL can move close to the target which is a three-dimensional spatially-periodic structure or through the target. In the common case an electron beam with initial electron velocity $\mathbf{u}$ and density n_b can pass at some angle through the target of the length L. Under diffraction conditions, strong coupled waves are generated. Under Cherenkov condition, electrons of the beam group in a deceleration phase and produce stimulated emission. In the case of amplification regime an external electromagnetic wave is incident to the target. Oscillator regime is realized without external waves. We discuss three-wave DVFB at present work. There are three possible geometries in such a system (see Fig. 1- 3). They will be discussed below.

The system of equations for the case of three-wave VFEL is obtained in the slowly-varying envelope approximation similar to two-wave system

[4] and can be written in the following form:

$$\frac{\partial E_0}{\partial t} + \gamma_0 c \frac{\partial E_0}{\partial z} + 0.5 i\omega l E_0 - 0.5 i\omega \chi_1 E_1 - 0.5 i\omega \chi_2 E_2$$

$$= 2\pi e j \Phi \int_0^{2\pi} \frac{2\pi - p}{8\pi^2} \left(\exp(-i\Theta(t,z,p) + \exp(-i\Theta(t,z,-p))\right) dp, \tag{2}$$

$$\frac{\partial E_1}{\partial t} + \gamma_1 c \frac{\partial E_1}{\partial z} - 0.5 i\omega \chi_{-1} E_0 + 0.5 i\omega l_1 E_1 - 0.5 i\omega \chi_{2-1} E_2 = 0, \tag{3}$$

$$\frac{\partial E_2}{\partial t} + \gamma_2 c \frac{\partial E_2}{\partial z} - 0.5 i\omega \chi_{-2} E_0 - 0.5 i\omega \chi_{1-2} E_1 + 0.5 i\omega l_2 E_2 = 0, \tag{4}$$

$$\frac{d^2\Theta(t,z,p)}{dz^2} = \frac{e\Phi}{m\gamma^3\omega^2} \left(k - \frac{d\Theta(t,z,p)}{dz}\right)^3 \Re e \left(E_0(t - z/u, z) \exp(i\Theta(t,z,p))\right), \tag{5}$$

$$\begin{gathered} \frac{d\Theta(t,0,p)}{dz} = k - \omega/u, \quad \Theta(t,0,p) = p, \\ E_0|_{z=0} = E_0^0, \quad E_1|_{z=L_1} = E_1^0, \quad E_2|_{z=L_2} = E_2^0, \\ E_m|_{t=0} = 0, \quad m = 0,1,2; \\ t > 0, \quad z \in [0, L], \quad p \in [-2\pi, 2\pi]. \end{gathered} \tag{6}$$

Here $E_0(t,z)$, $E_1(t,z)$, $E_2(t,z)$ are complex-valued amplitudes of three electromagnetic waves. $\Theta(t,z,p)$ describes the phase of electron beam relative to the electromagnetic wave, γ is the Lorentz-factor of a beam, e, m are electron charge and mass respectively. γ_j are direction cosines, $\beta_{1,2} = \gamma_0/\gamma_{1,2}$ are diffraction asymmetry factors.

$$l = l_0 + \delta,$$

δ is a tuning parameter from the Cherenkov condition. l_0, l_1, l_2 are system parameters corresponding to three waves:

$$l_i = \frac{\mathbf{k}_i^2 c^2 - \omega^2 \varepsilon_0}{\omega^2}.$$

ε_0 is the dielectric susceptibility and $\chi_{\pm j}$ are Fourier components of the dielectric susceptibility of the target.

$$\Phi = \sqrt{l_0 + \chi_0 - 1/(\beta\gamma)^2}.$$

Numerical methods for simulation of the systems analogous to the system (2)-(6) are presented in [5].

4 Different regimes of VDBF

Dispersion equation corresponding (2)-(4) reads:

$$l_0 l_1 l_2 - l_0 r_{12} - l_1 r_2 - l_2 r_1$$

$$-\chi_1 \chi_{-2} \chi_{2-1} - \chi_2 \chi_{-1} \chi_{1-2} = 0 \tag{7}$$

In two-root degeneration mode, besides (6) an additional condition

$$\beta_1\beta_2 l_1 l_2 + (\beta_1 l_1 + \beta_2 l_2) l_0$$

$$-\beta_1\beta_2 r_{12} - \beta_1 r_1 - \beta_2 r_2 = 0, \tag{8}$$

should be fulfilled. Here $r_1 = \chi_{-1}\chi_1$, $r_2 = \chi_{-2}\chi_2$, $r_{12} = \chi_{2-1}\chi_{1-2}$.

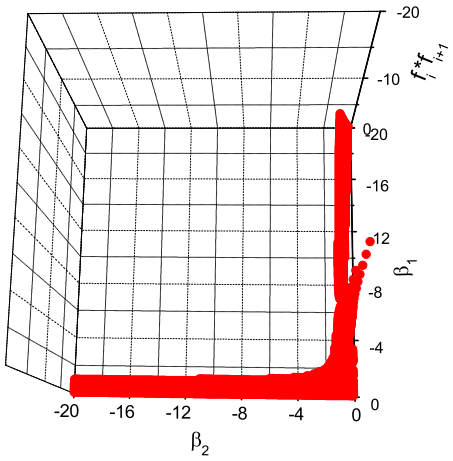

FIG. 4. Three-root degeneration points, $l_1 < 0$

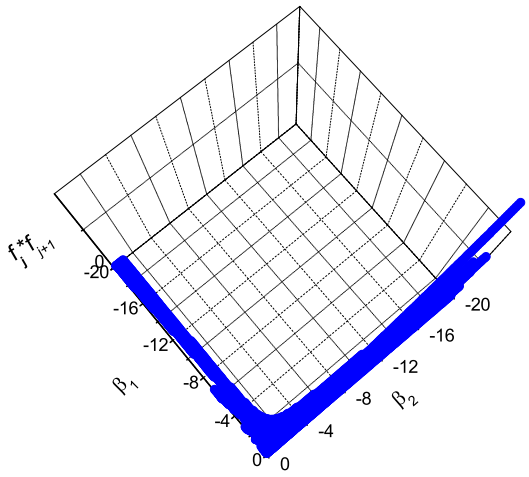

FIG. 5. Three-root degeneration points, $l_1 > 0$

Extra equation

$$\beta_2 l_2 + \beta_1 l_1 + l = 0 \qquad (9)$$

corresponds to generation in three root degeneration mode. Each subsequent equation narrows the domain of permissible parameters. Permissible values of diffraction asymmetry factors β_1 and β_2 generation in three-root degeneration mode are adduced in Fig. 4 for the case when $l_1 < 0$ and $l_1 > 0$ in Fig. 5. Figure corresponds to Bragg-Bragg geometry when one wave propagates in electron beam velocity direction and two others are in opposite direction (Fig. 1). It is evident the symmetry relative both factors.

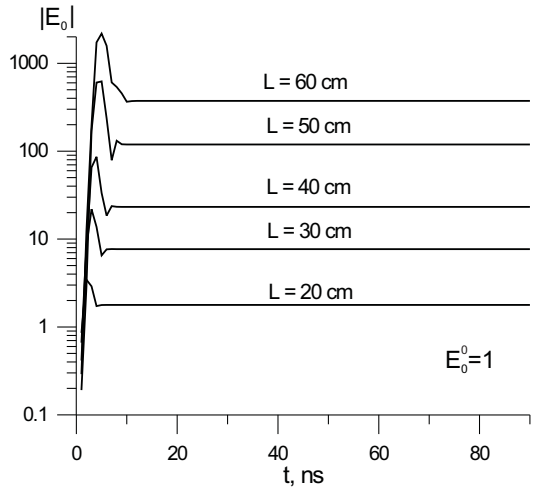

FIG. 6. Laue-Laue VFEL: numerical solution for different length L of the target

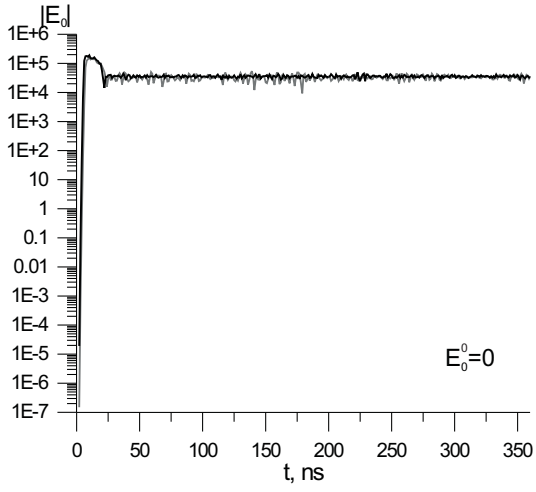

FIG. 7. SASE simulation for different numerical grid dimensions

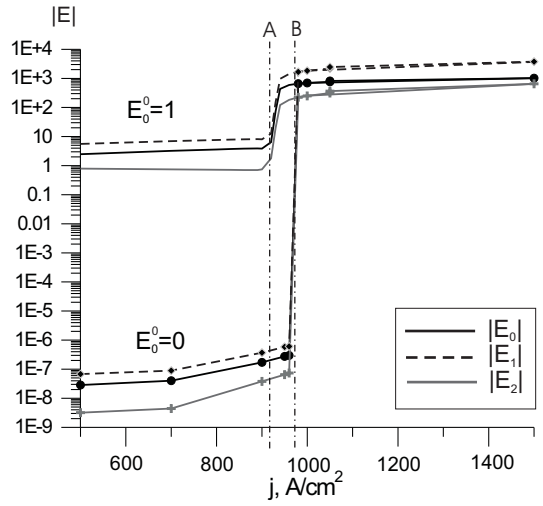

FIG. 8. Regimes of amplification and oscillation in Bragg-Laue geometry

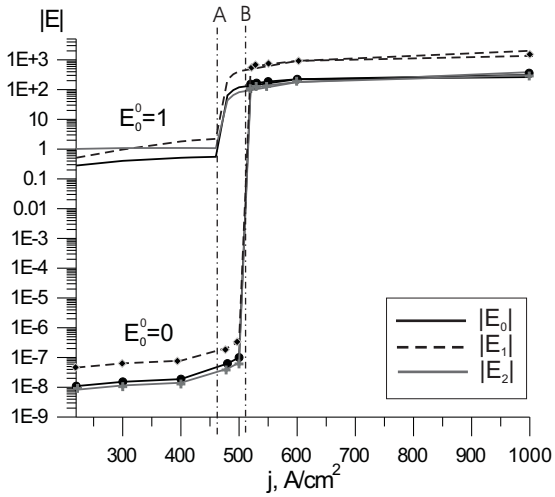

FIG. 9. Regimes of amplification and oscillation in Bragg-Bragg geometry

Let us consider different cases of VDFB. Laue-Laue geometry (Fig. 2) is realized when all three waves propagate in the same direction which corresponds to electron velocity direction. Dispersion equation (7) has no degeneration points in this case.

Two regimes of beam instability can be realized in this geometry: amplification of incident radiation and SASE (Self-Amplified Spontaneous Emission) regime. At amplification incident radiation grows

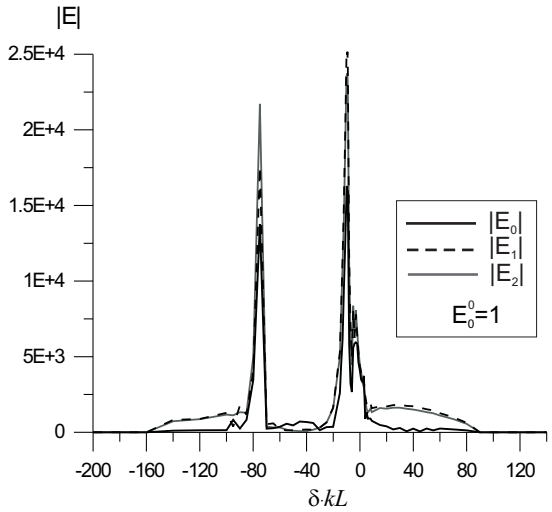

FIG. 10. One-root degeneration case: dependance on tuning parameter δ

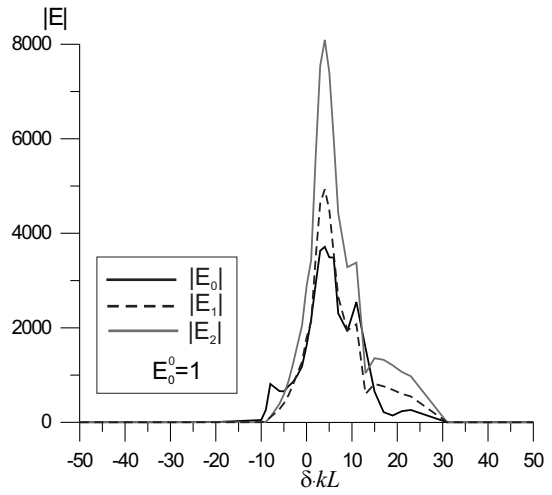

FIG. 11. Two-root degeneration case: dependance on tuning parameter δ

exponentially along the beam on linear interaction stage. Linear interaction transits to the nonlinear one at the saturation regime. Amplification level depends on energy transmitted from electrons to radiation to the moment of system transition to saturation. VFEL operation in such a

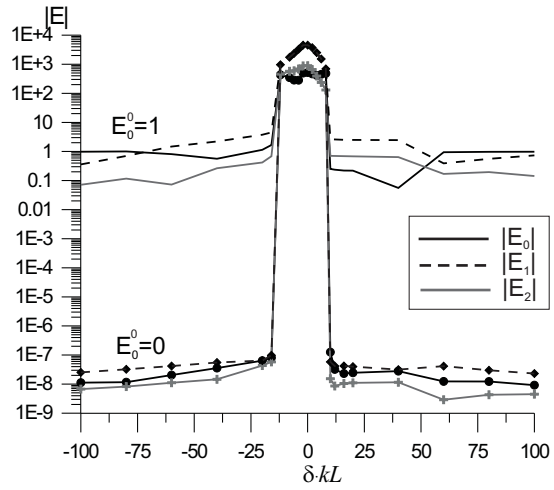

FIG. 12. Three-root degeneration case: dependance on tuning parameter δ

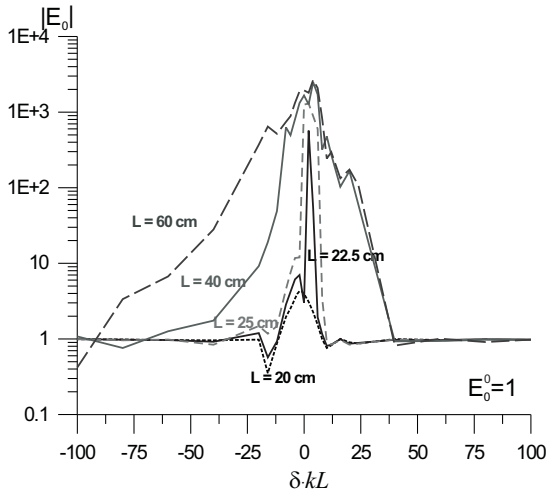

FIG. 13. Three-root degeneration case: dependance on tuning parameter δ for different L in Bragg-Laue geometry

geometry corresponds to so-called TWT (travelling wave tube) operation and is shown in Fig. 6.

SASE regime corresponds to generation without external incident radiation. It requires larger interaction length for shot noise can rise. In computer simulation computational error in right-hand side corresponds to this noise. And we showed good numerical stability of algorithms realized, the growth rate in calculations does not depend strongly on numerical grid points (see Fig. 7. One curve corresponds to very small grid dimensions, another one corresponds to sufficient grid dimensions and doesn't vary with increasing.

Bragg-Laue geometry (Fig. 3) is the case when two wave vectors are oriented along the direction of electron beam velocity and one wave is in the opposite direction. In this case additional possibilities for realizing of beam instability regime are possible. If beam current reaches first threshold point when radiation gain exceeds radiation loss, but at the same time is less than the second threshold point of generation, the regenerative amplification takes place. After a current reaches the second threshold point oscillations develop. This is depicted in Fig. 8. Lines A and B correspond to the first and second threshold points respectively. Analogous results for the Bragg-Bragg case are presented in Fig. 9.

In Bragg-Bragg and Bragg-Laue geometries generation regimes are possible also when two modes are in synchronism with electron beam. This corresponds to instability in the region of two roots degeneration as in two-wave diffraction geometry.

However in three-wave case additional parameters exist which give possibility to adjust generation to more optimal region. Besides three-wave distributed feedback can be realized in the region of three root degeneration. In this case all three modes are in synchronism with electron beam and interaction occurs more intensively. It gives possibility to realize oscillation at more compact spatial region.

In Fig. 10 - 12 dependence of numerical solution on tuning parameter δ is shown for one-, two- and three-root degeneration points respectively. In Fig. 13 one can see how the curve behavior is changed in dependance of length L for Bragg-Laue case.

In conclusion in Fig. 14 the periodic regime of VFEL intensity for Bragg-Bragg geometry and corresponding phase space portrait (Fig. 15) are given. It is evident that we deal with periodic 1T and 2T regimes. In SASE simulation (see Fig. 7) we obtained typical chaotic regime of laser inten-

sity.

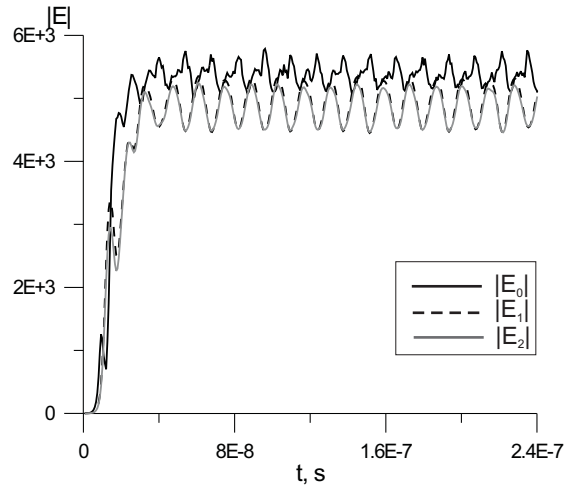

FIG. 14. Periodic regime of VFEL intensity for Bragg-Bragg geometry

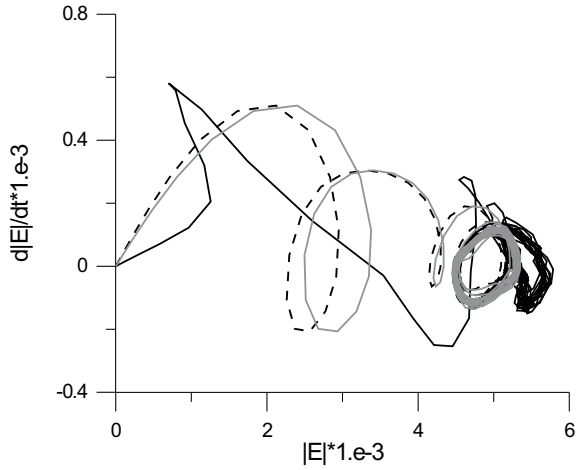

FIG. 15. Corresponding to Fig. 14 the phase space portrait

5 Conclusion

Different oscillation and amplification regimes of VFEL operation under condition of multiwave VDFB were demonstrated. Numerical results coincide completely with analytical estimations. They will be useful for further theoretical development and experiments on VFEL on the VFEL setup formed in the Institute for Nuclear Problems of Belarusian State University.

Acknowledgment

Authors thanks to prof. Baryshevsky for persistent interest to their work.

References

[1] V.G.Baryshevsky, I.D.Feranchuk. Parametric X-rays from ultrarelativistic electrons in a crystals: theory and possibilities of practical utilization. Phys.Let.A **102**, 141-144 (1984).

[2] V.G.Baryshevsky, K.G. Batrakov, I.Ya.Dubovskaya. Cherenkov instability of charged particles beam passing through three-dimensional spatial periodical medium. Proc. Nat. Academy Sci. Belarus. Ser. Phys.-Math. no. 2, 92-97 (1988).

[3] V.G.Baryshevsky, K.G.Batrakov et al. First lasing of a volume FEL (VFEL) at a wavelength range 4-6 mm. Nucl. Instr. Meth. Phys. Res. **A483**, 21-23 (2002).

[4] K.G.Batrakov, S.N.Sytova. Nonlinear analysis of quasi-Cherenkov electron beam instability in VFEL (Volume Free Electron Laser). Nonlinear Phenomena in Complex Systems. **8**, 42-48 (2005).

[5] K.G.Batrakov, S.N.Sytova. Modelling of Volume Free Electron Lasers. Comp. Math. and Math. Phys. **45**, 666-676 (2005).